AEM
Journals.ASM.org

# Minimum Requirements of Flagellation and Motility for Infection of *Agrobacterium* sp. Strain H13-3 by Flagellotropic Bacteriophage 7-7-1

**Jiun Y. Yen, Katherine M. Broadway, and Birgit E. Scharf**

Department of Biological Sciences, Virginia Tech, Blacksburg, Virginia, USA

**The flagellotropic phage 7-7-1 specifically adsorbs to *Agrobacterium* sp. strain H13-3 (formerly *Rhizobium lupini* H13-3) flagella for efficient host infection. The *Agrobacterium* sp. H13-3 flagellum is complex and consists of three flagellin proteins: the primary flagellin FlaA, which is essential for motility, and the secondary flagellins FlaB and FlaD, which have minor functions in motility. Using quantitative infectivity assays, we showed that absence of FlaD had no effect on phage infection, while absence of FlaB resulted in a 2.5-fold increase in infectivity. A *flaA* deletion strain, which produces straight and severely truncated flagella, experienced a significantly reduced infectivity, similar to that of a *flaB flaD* strain, which produces a low number of straight flagella. A strain lacking all three flagellin genes is phage resistant. In addition to flagellation, flagellar rotation is required for infection. A strain that is nonmotile due to an in-frame deletion in the gene encoding the motor component MotA is resistant to phage infection. We also generated two strains with point mutations in the *motA* gene resulting in replacement of the conserved charged residue Glu98, which is important for modulation of rotary speed. A change to the neutral Gln caused the flagellar motor to rotate at a constant high speed, allowing a 2.2-fold-enhanced infectivity. A change to the positively charged Lys caused a jiggly motility phenotype with very slow flagellar rotation, which significantly reduced the efficiency of infection. In conclusion, flagellar number and length, as well as speed of flagellar rotation, are important determinants for infection by phage 7-7-1.**

*Agrobacterium* sp. strain H13-3, formerly known as *Rhizobium lupini* H13-3, was isolated from the rhizosphere of *Lupinus luteus* (11). Its complete genome has been recently sequenced, and subsequent genome structure and phylogenetic analyses identified the strain as a nonpathogenic *Agrobacterium* strain (44). *Agrobacterium* sp. H13-3 is motile by means of peritrichously inserted flagella. Based on the microscopic appearance, there are two types of flagellar filaments in bacteria, plain and complex. The plain filaments of *Escherichia coli* have a smooth surface structure and are capable of switching from left-handed to right-handed helicity (22). The complex filaments of *Agrobacterium* sp. H13-3 and the related soil bacterium *Sinorhizobium meliloti* exhibit a dominant pattern of alternating ridges and grooves and do not switch handedness (18, 42, 43). The *E. coli* filament consists of a single type of flagellin, while the *Agrobacterium* sp. H13-3 filament consists of three related flagellin subunits, FlaA, FlaB, and FlaD, that are assembled as functional heterodimers (35). The C- and N-terminal regions of flagellins are required for assembly of the flagellum and are highly conserved among the three subunits. The central domains, defining the diverse surface of the filament, exhibit more sequence variability. FlaA is the primary flagellin, and a *flaA* deletion mutant produces severely truncated, straight flagella that appear to be unusually fragile. Since *flaB* and *flaD* deletion mutants exhibit a minor reduction in swimming speed and have a normal flagellar appearance, FlaB and FlaD are considered secondary flagellins. However, a strain carrying deletions in both secondary flagellin genes is nonmotile and produces a very low number of straight flagella. In conclusion, FlaA and at least one secondary Fla protein are required for the assembly of a flagellar filament that can promote motility (35).

Bacterial flagella are driven by a rotary motor at the flagellar base which is energized by a proton gradient across the cytoplasmic membrane (23). The flagellar motors of *E. coli* switch their sense of rotation, which enables them to change direction (21). The complex filaments are more rigid, because interflagellin bonds lock the filament in a right-handed helical conformation (6). The rigidity of these filaments allows propulsion with a greater force in viscous media (12). Concomitantly, *Agrobacterium* sp. H13-3 and *S. meliloti* flagellar motors rotate exclusively clockwise and direct the swimming path by modulating their rotary speed (1, 34). This swimming behavior requires the activity of two novel motility proteins, MotC and MotE, which are present in addition to the ubiquitous proton channel-forming MotA and MotB. MotC binds to the periplasmic portion of MotB, whereas MotE serves as its periplasmic chaperone (8).

Flagellotropic bacteriophages specifically target bacterial flagella and require motility of the host for a productive infection. They adsorb to the host's flagella and then proceed to the cell membrane, where the phage DNA is injected. This phage family is represented by χ of *E. coli* and *Serratia marcescens*, ΦCB13 and ΦCbK of *Caulobacter crescentus*, PBS1 and SP3 of *Bacillus subtilis*, ΦAT1 of *Erwinia carotovora* (10), Φ OT8 of *Serratia* sp. strain ATCC 39006 and *Pantoea agglomerans*, and 7-7-1 of *Agrobacterium* sp. H13-3 (9, 13, 15, 16, 19, 28, 30–32). Since not the mere presence of flagella but their rotation is essential for infection, a "nut-and-bolt" model for the translocation of phage along the filament was suggested. The tail fiber of the *E. coli* χ phage fits the right-handed helical grooves on the flagellar surface, and counterclockwise rotation would force the phage to follow the grooves to the base of the flagellar filament (3, 31). Bacteriophage 7-7-1 was isolated from composed soil in Germany in the 1970s (20). It is a member of the *Myoviridae* family, consisting of a hexagonal head

**Received** 3 April 2012 **Accepted** 27 July 2012
**Published ahead of print** 3 August 2012
Address correspondence to Birgit E. Scharf, bscharf@vt.edu.

doi:10.1128/AEM.01082-12

**TABLE 1** Bacterial strains and plasmid

| Species and strain or plasmid | Relevant characteristics[a] | Source or reference |
|---|---|---|
| *E. coli* | | |
| DH10B | *recA1 endA1* | GIBCO/BRL |
| S17-1 | *recA endA thi hsdR* RP4-2 Tc::Mu::Tn*7* $Tp^r$ $Sm^r$ | 38 |
| *Agrobacterium rhizogenes* ATCC 11325 | | Bertrand Eardly |
| *Agrobacterium rubi* ATCC 13335 | | Bertrand Eardly |
| *Agrobacterium* sp. H13-3 | | |
| RU12/001 | $Sm^r$; spontaneous streptomycin-resistant wild-type strain | 35 |
| RU12/002 | $Sm^r$; Δ*flaA* | 35 |
| RU12/003 | $Sm^r$; Δ*flaB* | 35 |
| RU12/004 | $Sm^r$; Δ*flaD* | 35 |
| RU12/005 | $Sm^r$; Δ*flaB* Δ*flaD* | 35 |
| RU12/006 | $Sm^r$; Δ*flaA* Δ*flaB* Δ*flaD* | 35 |
| RU12/010 | $Sm^r$; *motA*E98K | This work |
| RU12/011 | $Sm^r$; *motA*E98Q | This work |
| RU12/012 | $Sm^r$; Δ*motA* | This work |
| *Agrobacterium tumefaciens* C58 | | Clay Fuqua |
| *Agrobacterium vitis* ATCC 49767 | | Bertrand Eardly |
| *Rhizobium etli* ATCC 51251 | | Bertrand Eardly |
| *Rhizobium galegae* ATCC 43677 | | Bertrand Eardly |
| *Rhizobium leguminosarum* biovar *viciae* 3841 | $Sm^r$ | Gladys Alexandre |
| *Rhizobium tropici* ATCC 49672 | | Joshua Shrout |
| Plasmid pK18*mobsacB* | $Km^r$; *lacZ mob sacB* | 33 |

[a] Nomenclature is according to Bachmann (2) and Novick et al. (25).

and a tail separated by a neck (5). The diameter of the head is 68 nm, and the phage tail has a length of 135 nm and a diameter of 20 nm. The tail is contractile and ends in bushy fibers (19, 20). 7-7-1 is a lytic phage which specifically infects *Agrobacterium* sp. H13-3 but not the closely related *S. meliloti*, which also possesses complex flagella (19). The eclipse period lasts approximately 60 min, and the complete cycle of phage propagation takes 80 min, with a burst size of 120 particles per bacterial cell (19, 41). Phage-resistant *Agrobacterium* sp. H13-3 mutants were selected after chemical mutagenesis, and most of these were nonflagellated. In addition, a small percentage of mutants were found to be nonmotile (19). Therefore, flagella and motility seem to be essential for the infection of *Agrobacterium* sp. H13-3 by phage 7-7-1. However, it is yet unknown how the phage attaches to the flagellum and reaches the bacterial cell surface.

In this study, we determined flagellation and flagellar rotation as requirements for infection of *Agrobacterium* sp. H13-3 by bacteriophage 7-7-1. Defined deletion and amino acid exchange mutants of *Agrobacterium* sp. H13-3 were constructed by allelic exchange, and the infectivity of bacteriophage 7-7-1 for the resulting flagellar and motility mutants was quantified. Requirements for the infection of *Agrobacterium* sp. H13-3 are discussed.

## MATERIALS AND METHODS

**Bacterial strains and plasmids.** Derivatives of *E. coli* K-12 and *Agrobacterium* sp. H13-3 (17), *Agrobacterium* and *Rhizobium* strains, and the plasmids used are listed in Table 1.

**Media and growth conditions.** *E. coli* strains were grown in LB at 37°C (4). *Agrobacterium* and *Rhizobium* strains were grown in TYC (0.5% tryptone, 0.3% yeast extract, 0.13% $CaCl_2 \cdot 6H_2O$ [pH 7.0]) or TYC40 (0.2% tryptone, 0.13% yeast extract, 0.05% $CaCl_2 \cdot 6H_2O$ [pH 7.0]), as indicated, at 30°C (27). Cells for motility assays were diluted in 10 ml RB minimal medium [6.1 mM $K_2HPO_4$, 3.9 mM $KH_2PO_4$, 1 mM $MgSO_4$, 1 mM $(NH_4)_2SO_4$, 0.1 mM $CaCl_2$, 0.1 mM NaCl, 0.01 mM $Na_2MoO_4$, 0.001 mM $FeSO_4$, 20 μg $l^{-1}$ biotin, and 100 μg $l^{-1}$ thiamine] (12), layered on Bromfield agar plates (40), and incubated at 30°C for 14 h. The following antibiotics were used at the indicated final concentrations in LB or TYC medium: for *E. coli*, kanamycin at 50 μg $ml^{-1}$, and for *Agrobacterium* sp. H13-3, neomycin at 120 μg $ml^{-1}$ and streptomycin at 600 μg $ml^{-1}$.

**Culture lysis assays.** Cultures were grown in TYC40 from single colonies at 30°C for 18 to 26 h until they reached an optical density at 600 nm ($OD_{600}$) of 0.3. For each strain, two cultures were adjusted to an $OD_{600}$ of 0.03 with TYC40; one was incubated with bacteriophage 7-7-1 at a multiplicity of infection (MOI) of 1.0, and the second was incubated as a control in a shaking incubator at 220 rpm at 30°C. $OD_{600}$ readings were recorded after 24 h, and each experiment was run in triplicates.

**Phage drop assays.** Swim plates containing Bromfield medium and 0.3% Bacto agar were inoculated with a single colony using a toothpick and incubated at 30°C until the swim ring reached a diameter of 2 cm (typically 1 to 2 days). Two microliters of a phage stock of $2 \times 10^{11}$ in 0.85% NaCl was carefully pipetted on the outside edge of the swim ring, and 2 μl of 0.85% NaCl was pipetted on the opposite side of the swim ring as a control (see Fig. 2A). Plates were observed and documented every 24 h until swim rings reached a diameter of approximately 6 cm.

**Infectivity assays.** Infectivity assays were performed essentially as described by Lotz et al. (19) with a few minor modifications. *Agrobacterium* strains grown in TYC overnight at 30°C were adjusted to an $OD_{600}$ of 0.3 in TYC, and incubated with bacteriophage 7-7-1 at an MOI of 0.01 (20) in a shaking incubator for 15 min at 30°C, and then diluted to $10^{-3}$ in TYC and incubated further. At 0.5, 1, 2, 3, and 4 h after infection, 100-μl aliquots were withdrawn, 5 ml 0.85% NaCl and 100 μl chloroform were added, and the mixture was vortexed vigorously for 60 s. Serial dilutions were plated by mixing 100 μl of wild-type *Agrobacterium* sp. H13-3 as the indicator strain with 4 ml molten TYC and 0.5% Bacto agar, layered on TYC plates, and incubated overnight at 30°C. PFU were normalized to the 30-min time point of strain RU12/001.

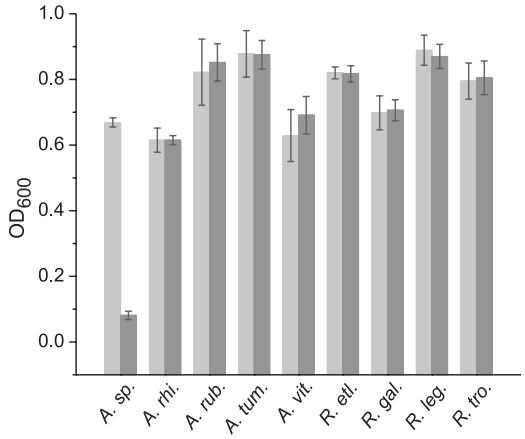


**FIG 1** Optical densities of cultures grown for 24 h at 30°C in the absence and presence of phage 7-7-1. *A.* sp., *Agrobacterium* sp. H13-3; *A. rhi.*, *A. rhizogenes*; *A. rub.*, *A. rubi*; *A. tum.*, *A. tumefaciens*; *A. vit.*, *A. vitis*; *R. etl.*, *R. etli*; *R. gal.*, *R. galegae*; *R. leg.*, *R. leguminosarum*; *R. tro.*, *R. tropici*. Motile cultures were adjusted to an $OD_{600}$ of 0.03, and phage 7-7-1 was added to an MOI of 1.0. Light and dark gray bars depict cultures grown in the absence and presence of phage, respectively. Each bar represents the average from three independent experiments, and error bars represent standard deviations (Student's *t* test for *Agrobacterium* sp. H13-3, $P < 0.001$).

**Motility assays.** Swim plates containing Bromfield medium and 0.3% Bacto agar were inoculated with 3-μl droplets of the test culture and incubated at 30°C for 3 days. Motile cell samples were observed with a Nikon Eclipse E600 phase-contrast microscope. Tracks of swimming cells were determined by computerized motion analysis using the Hobson Bactracker system (Hobson Tracking System Ltd., Sheffield, United Kingdom) as previously described (40).

**DNA methods and genetic manipulations.** *S. meliloti* DNA was isolated and purified as described previously (40). Plasmid DNA was purified with NucleoSpin (Macherey-Nagel, Düren, Germany) or the Wizard Plus SV Miniprep system (Promega). DNA fragments or PCR products were purified from agarose gels using a GFX PCR and gel band purification kit (GE Healthcare) or the Wizard SV gel and PCR clean-up system (Promega).

Deletion constructs and codon exchanges were generated using the overlap extension PCR method described by Higuchi (14). These constructs were cloned into the mobilizable suicide vector pK18*mobsacB*, which was then used to transform *E. coli* S17-1, and conjugally transferred to *S. meliloti* by filter mating according to the method of Simon et al. (37). Allelic replacement was achieved by sequential selections on neomycin and 10% sucrose as described previously (40). Confirmation of allelic replacement and elimination of the vector was obtained by gene-specific primer PCR and DNA sequencing.

## RESULTS

**Bacteriophage 7-7-1 does not infect closely related *Rhizobiaceae*.** Analysis of the *Rhizobium lupini* H13-3 genome sequence identified the strain as a nonpathogenic *Agrobacterium* strain, and the organism has therefore been renamed *Agrobacterium* sp. H13-3. The flagellotropic bacteriophage 7-7-1 is known to specifically infect *Agrobacterium* sp. H13-3 but not related soil bacteria with complex flagella, such as *Sinorhizobium meliloti* and *Methylobacterium rhodinum* (formerly *Pseudomonas rhodos*) (36). To uncover detailed information about the host range of phage 7-7-1, we tested eight species from the *Rhizobiaceae* family that are closely related to *Agrobacterium* sp. H13-3 (7), namely, *Agrobacterium rhizogenes*, *Agrobacterium rubi*, *Agrobacterium tumefaciens*, *Agrobacterium vitis*, *Rhizobium etli*, *Rhizobium galegae*, *Rhizobium leguminosarum*, and *Rhizobium tropici*. We used a broth-based assay to observe phage-induced bacterial lysis. To establish a common growth medium that allowed all nine different species to develop optimal motility, we tested media with different concentrations of TYC (tryptone-yeast extract-$CaCl_2$). Most consistently, all strains were highly motile in TYC medium with a lower concentration of nutrients (40%) than our standard TYC (TYC40). Using phase-contrast microscopy, we observed that 90% of cells in cultures grown to an $OD_{600}$ of 0.3 were motile. These cultures were diluted with fresh medium, phage was added at a multiplicity of infection (MOI) of 1.0, and the optical density was determined after 24 h of growth (Fig. 1). The OD of *Agrobacterium* sp. H13-3 cultures grown in the presence of phage was 10-fold lower than the OD of cultures grown in the absence of phage, showing phage-induced bacterial lysis. The eight remaining strains grew equally well in the absence or presence of phage, indicating that they were not infected by 7-7-1. We also developed a second, qualitative assay, named the "phage drop assay," to demonstrate phage-induced bacterial lysis. This assay takes place in swim plates, where cells consume the carbon source at the inoculation point and migrate toward higher concentrations, thereby forming a swim ring (24, 45). We allowed the formation of a swim ring with a diameter of 2 cm for each of the nine strains before colonies were infected with phage. Figure 2A shows *Agrobacterium* sp. H13-3 at the time of inoculation and depicts the inoculation procedure. Over time, swim ring development could be observed for all strains, but only *Agrobacterium* sp. H13-3 cells were lysed at

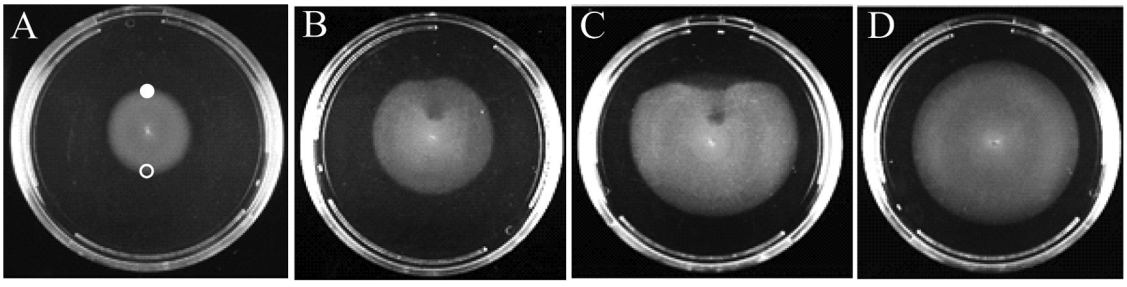


**FIG 2** Phage drop assay for *Agrobacterium* H13-3 and *A. tumefaciens* C58. Single colonies were transferred with a toothpick onto a Bromfield swim plate and incubated at 30°C. Phage and control drops were applied when swim rings reached a diameter of 2 cm. (A) *Agrobacterium* H13-3 RU12/001 at time zero of infection. The closed and open circles (not drawn to scale) depict the positions of the phage drop (2 μl of a phage stock of $2 \times 10^{11}$ in 0.85% NaCl) and control drop (2 μl 0.85% NaCl), respectively. (B) *Agrobacterium* H13-3 RU12/001 after 2 days of infection. (C) *Agrobacterium* H13-3 RU12/001 after 4 days of infection. (D) *A. tumefaciens* C58 after 2 days of infection.

and around the phage inoculation point (Fig. 2B and C). In comparison, the swim ring of *A. tumefaciens* C58 at 2 days after phage infection is shown in Fig. 2D. The funnel-shaped lysis pattern of *Agrobacterium* sp. H13-3 reflects phage diffusion but, most importantly, outward movement of infected cells before cell lysis. In addition, a quantitative infectivity assay was performed for *Agrobacterium* sp. H13-3 and its closest relative, *A. tumefaciens*. Phage 7-7-1 was added to an exponentially growing bacterial culture at an MOI of 0.01, and phage growth was followed over time. Upon the infection of *Agrobacterium* sp. H13-3, we observed phage growth after a latent period of about 60 min (Fig. 3A), which is in agreement with previously published results (19). When *A. tumefaciens* was infected, the number of phage particles in the culture did not increase (Fig. 3A). The initial decrease of PFU for *Agrobacterium* H13-3 compared to *A. tumefaciens* is explained by immediate phage adsorption and DNA injection into the host cell and therefore loss of active phage particles. In conclusion, the host range of phage 7-7-1 is confined to *Agrobacterium* H13-3.

**The number and length of flagella are important determinants of infectivity.** The adsorption of bacteriophage 7-7-1 to flagellar filaments is an essential prerequisite for infection (19). We therefore analyzed whether infection is affected by two flagellar parameters, namely, number and length. We tested the susceptibilities of five flagellar mutants to infection by 7-7-1 and compared the obtained data to those for the wild type. Genotype and flagellation characteristics of the mutant strains are summarized in Table 2. Deletion of either of the secondary flagellin genes, *flaB* or *flaD*, did not have a negative effect on phage infection. In fact, phage propagation increased 2.5-fold in the *flaB* deletion strain (Fig. 3B; Table 2). Cells lacking the primary flagellin gene, *flaA* (strain RU12/002), produce severely truncated and straight flagella (35), and as a consequence, a 3-fold decrease in phage titer was observed. With a 10-fold decrease in phage titer, this trend was even more pronounced in strain RU12/005, which lacks both secondary flagellins (Fig. 3B; Table 2). Very few RU12/005 cells were flagellated, and the few flagellar filaments exhibited an improper helical structure (35). Finally, a strain lacking all three flagellin genes was resistant to phage infection. In conclusion, the number and length of flagellar filaments are important determinants of infectivity by 7-7-1.

**Minimal flagellar rotation is sufficient to promote infection.** In addition to flagellation, flagellar rotation is another parameter required for efficient infection by flagellotropic phages (19). We therefore analyzed whether infection is affected by the rotational speed of flagellar filaments. The flagellar motors of *S. meliloti* and *Agrobacterium* sp. H13-3 can modulate their rotary speed in response to tactic stimuli (1, 12). Two conserved charged amino acid residues in the motor protein MotA, Arg90 and Glu98, are essential for speed modulation. In *S. meliloti*, a replacement of Glu98 with the charge-neutralizing Gln caused an increase in swimming speed (1). The same mutation was introduced into *Agrobacterium* sp. H13-3, and the resulting mutant strain, RU12/011, also showed an increase in swimming speed (data not shown). When a qualitative infectivity assay was performed, a modest, 2.2-fold increase in phage propagation was observed (Fig. 3C; Table 2). The effect of another mutation in *motA*, replacement of Glu98 by a positively charged Lys, was also analyzed. In *S. meliloti*, this substitution led to a complete loss of motility (1). When we analyzed the swimming behavior of the identical *Agrobacterium* sp. H13-3 mutant strain (RU12/010) on swim plates, the cells

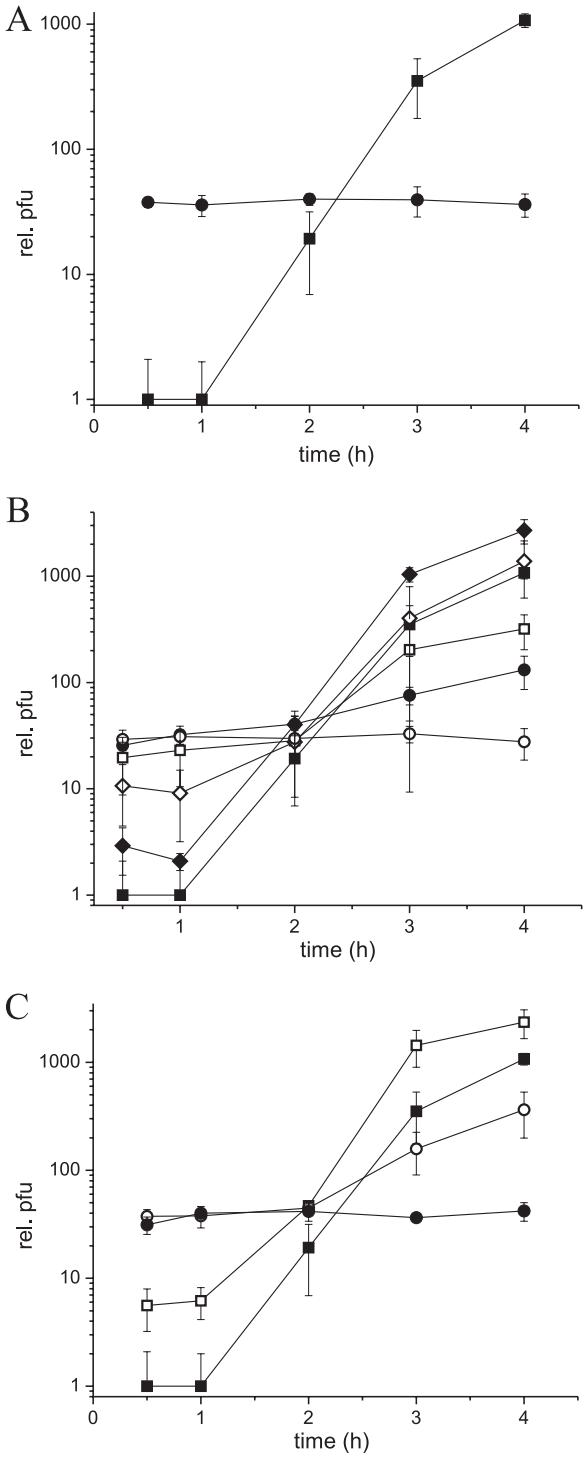


**FIG 3** Bacteriophage growth after addition of phage 7-7-1 to bacterial cultures. (A) *Agrobacterium* sp. H13-3 (■) and *Agrobacterium tumefaciens* (●). (B) *Agrobacterium* sp. H13-3 wild-type cells (■) and flagellar mutant cells: Δ*flaA* (□), Δ*flaB* (◆), Δ*flaD* (◇), Δ*flaBD* (●), and Δ*flaABD* (○). (C) *Agrobacterium* sp. H13-3 wild-type cells (■) and motility mutant cells; *mot*AE98K (○), *mot*AE98Q (□), and Δ*motA* (●). Cultures were adjusted to an $OD_{600}$ of 0.3, corresponding to $3.5 \times 10^8$ cells/ml, and phage 7-7-1 was added at an MOI of 0.01. After 15 min of phage adsorption, the mixtures were diluted 1:1,000 and incubated further at 30°C. Samples were taken at 1-h intervals, and PFU were determined by the soft agar layer technique. Each data point represents the average from three independent experiments, and error bars represent standard deviations.

TABLE 2 Properties of *Agrobacterium* sp. H13-3 *fla* and *mot* mutants

| Strain | Genotype | Flagellar morphology[a] | Motor rotation[a] | Relative phage sensitivity (mean ± SD)[b] |
|---|---|---|---|---|
| RU12/001 | Wild type | Normal | Normal | 1.00 ± 0.12 |
| RU12/002 | Δ*flaA* | Straight, truncated | Normal | 0.30 ± 0.11 |
| RU12/003 | Δ*flaB* | Normal | Normal | 2.52 ± 0.26 |
| RU12/004 | Δ*flaD* | Normal | Normal | 1.29 ± 0.27 |
| RU12/005 | Δ*flaB* Δ*flaD* | Straight, low numbers | Normal | 0.12 ± 0.04 |
| RU12/006 | Δ*flaA* Δ*flaB* Δ*flaD* | No flagella | Normal | 0.03 ± 0.01 |
| RU12/010 | *mot*AE98K | Normal | Slow | 0.34 ± 0.15 |
| RU12/011 | *mot*AE98Q | Normal | Fast | 2.19 ± 0.29 |
| RU12/012 | Δ*motA* | Normal | Immotile | 0.04 ± 0.01 |

[a] Data for RU12/001 to RU12/006 are from reference 35.
[b] Numbers of phage particles detected after 4 h of culture growth compared to numbers after growth on the wild type.

grew only at the inoculation point and did not generate a swim ring, indicating the predicted immotile phenotype (Fig. 4A). However, RU12/010 was not found to be resistant to phage as expected for a nonmotile strain, but instead, phage propagation exhibited only a 3-fold decrease compared to that for the wild type (Fig. 4C; Table 2). When we examined the strain using phase-contrast microscopy, we observed jiggly movement with some spatial displacement (Fig. 4C), which was slightly larger than the Brownian motion of a nonmotile strain (Fig. 4D). In addition, a spontaneously tethered cell (Fig. 4C, inset) showed slow rotational movement. Although the mutant had severely impaired motility, the flagellar filaments were still able to rotate. This slow rotation allowed the infection by 7-7-1. To show that a nonmotile mutant is indeed phage resistant, we introduced an in-frame deletion in the *motA* gene. The resulting mutant, RU12/012, was immotile on swim plates (Fig. 4A) and during microscopic observation (Fig. 4D). Furthermore, RU12/012 showed resistance toward 7-7-1 (Fig. 3C; Table 2). In conclusion, flagellar rotation is required for infection, slow flagellar rotation reduces infection efficiency 3-fold, and fast flagellar rotation increases infection efficiency 2.2-fold.

## DISCUSSION

Successful infection of bacterial cells by bacteriophages depends on the presence of bacterial cell surface receptors such as membrane proteins and lipopolysaccharides (26, 29, 39). The use of the bacterial flagellum as a primary receptor for phage attachment is rare (9, 10, 19, 31, 32). Infection by flagellotropic phage is often species specific; χ infects *E. coli* and *Serratia marcescens* (15, 31, 32), and as shown in this study, 7-7-1 infects only *Agrobacterium* sp. H13-3 and not closely related *Rhizobiaceae* (Fig. 1 and 2). The requirements for infection of *E. coli* by χ phage are counterclockwise rotation of the flagellum and appropriate dimensions of the right-handed surface grooves on the flagellar filament, suggesting a nut-and-bolt mechanism for phage movement along the filament (31). Similarly, active clockwise rotation of the *Agrobacterium* sp. H13-3 flagellum is essential for infection by 7-7-1 (Fig. 3). Here, we analyzed the requirements of flagellar structure and rotation in more detail.

We observed a clear correlation between infectivity and flagellar length and number. Mutant strains expressing flagella severely reduced with regard to number or length exhibited an overall reduction of infectivity of 70 to 90% (Table 2). However, phage 7-7-1 was able to locate these reduced structures, suggesting a high affinity to the flagellar filament. Since straight flagellar rods, as produced by *flaA* and *flaB flaD* deletion strains, were still promoting infection, the overall flagellar shape was not important. We have shown previously that these straight flagellar filaments exhibit a pattern of helical ridges and grooves (35). Therefore, and as reported for χ phage, the correct structure of helical grooves on the surface of the filament is important for infection (31). Interestingly, individual deletions of the secondary flagellin genes *flaB* and *flaD* led to a modest increase in infectivity (Table 2). We speculate that the FlaA subunit is the primary docking site. If the density of this docking site is increased along the filament due to the absence of the secondary flagellin subunits, infection efficiency increases.

We also confirmed that rotation of the *Agrobacterium* sp. H13-3 wild-type filament is essential for infection by phage 7-7-1. An earlier study performed with spontaneous and mutagen-induced immotile mutants indicated the importance of flagellar ro-

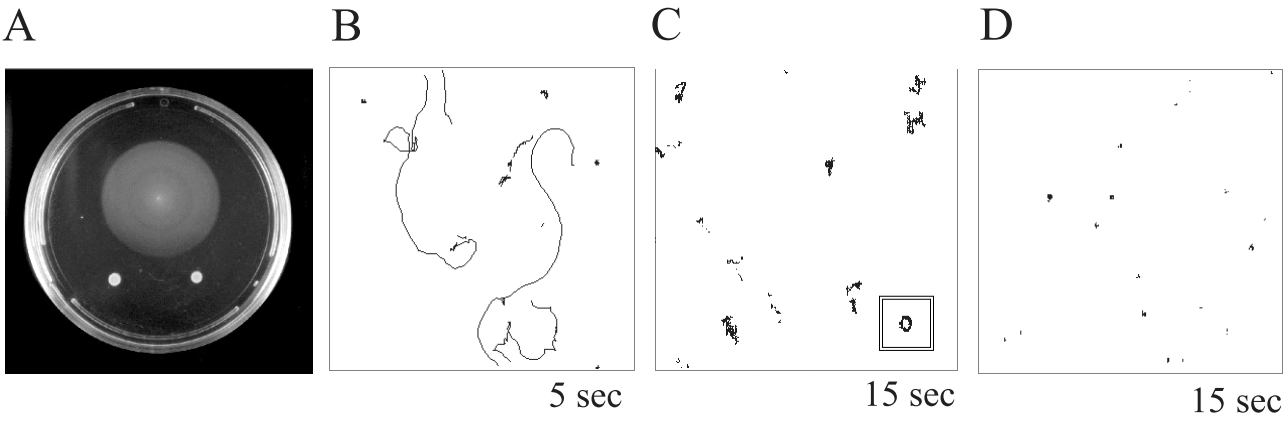


**FIG 4** Motility behavior of motility mutants compared to wild-type *Agrobacterium* sp. H13-3. (A) Swim test of wild-type (RU12/001) (top), *mot*AE98K (RU12/010) (bottom left), and Δ*motA* (RU12/012) (bottom right) *Agrobacterium* sp. H13-3. Strains to be tested were transferred with a micropipette (3 μl) onto Bromfield swim plates and incubated at 30°C for 2 days. The diameter of a swim ring reflects the motility of a given strain. (B to D) Swimming paths of wild-type *Agrobacterium* sp. H13-3 RU12/001 (B), *mot*AE98K RU12/010 (C), and Δ*motA* RU12/012 (D). Swimming cells were monitored by computerized motion analysis. The inset in Fig. 2C represents the rotational path of a cell spontaneously tethered to the coverslip by one of its flagellar filaments.

tation for infection (19). However, the experiments reported in that study were performed with a nondefined mutant. This led us to investigate the susceptibility of a *motA* deletion strain, and we found it to be phage resistant, confirming the previous study. Furthermore, we studied the correlation between speed of flagellar rotation and infection by using single point mutations in *motA*. Slow rotation of the flagellar filament, which was not sufficient to effectively propel the cells in an aqueous environment, still yielded a noticeable, but significantly reduced, infection (Fig. 3C and 4). In contrast, infection rates doubled for a mutant strain (1) with continuously fast flagellar rotation (Fig. 3C). While flagellar rotation is required for infection, the rotational speed apparently exerts a fine-tuning mechanism on infection rates.

The flagellar filament of *Agrobacterium* sp. H13-3 serves as the primary receptor for phage 7-7-1. Any reduction in the length or number of flagellar filaments decreases the efficiency of infection. The other determinant for an effective infection is active rotation of the flagellar filament. Moreover, infection rates are proportional to the rotational speed of the flagellum. Further physiological and structural studies are required to determine the exact mechanisms by which the phage binds to the flagellum, moves toward the cell surface, and infects the cell.

## ACKNOWLEDGMENTS

This study was supported by start-up funds from Virginia Tech.

We thank Robert Bourret for the use of the Hobson Tracker System, Gladys Alexandre, Bertrand Eardly, Clay Fuqua, and Joshua Shrout for the gifts of *Agrobacterium* and *Rhizobium* strains, and Benjamin Webb and Hardik Zatakia for critical reading of the manuscript.

## REFERENCES

1. **Attmannspacher U, Scharf B, Schmitt R.** 2005. Control of speed modulation (chemokinesis) in the unidirectional rotary motor of *Sinorhizobium meliloti.* Mol. Microbiol. **56**:708–718.
2. **Bachmann BJ.** 1990. Linkage map of *Escherichia coli* K-12, edition 8. Microbiol. Rev. **54**:130–197. (Erratum, **55**:191, 1991.)
3. **Berg HC, Anderson RA.** 1973. Bacteria swim by rotating their flagellar filaments. Nature **245**:380–382.
4. **Bertani G.** 1951. Studies on lysogenesis. I. The mode of phage liberation by lysogenic *Escherichia coli.* J. Bacteriol. **62**:293–300.
5. **Bradley DE.** 1967. Ultrastructure of bacteriophage and bacteriocins. Bacteriol. Rev. **31**:230–314.
6. **Cohen-Krausz S, Trachtenberg S.** 1998. Helical perturbations of the flagellar filament: *Rhizobium lupini* H13-3 at 13 Å resolution. J. Struct. Biol. **122**:267–282.
7. **Eardly BD, Nour SM, van Berkum P, Selander RK.** 2005. Rhizobial 16S rRNA and *dnaK* genes: mosaicism and the uncertain phylogenetic placement of *Rhizobium galegae*. Appl. Environ. Microbiol. **71**:1328–1335.
8. **Eggenhofer E, Haslbeck M, Scharf B.** 2004. MotE serves as a new chaperone specific for the periplasmic motility protein, MotC, in *Sinorhizobium meliloti.* Mol. Microbiol. **52**:701–712.
9. **Evans TJ, et al.** 2010. Characterization of a broad-host-range flagellum-dependent phage that mediates high-efficiency generalized transduction in, and between, *Serratia* and *Pantoea.* Microbiology **156**:240–247.
10. **Evans TJ, Trauner A, Komitopoulou E, Salmond GP.** 2010. Exploitation of a new flagellatropic phage of *Erwinia* for positive selection of bacterial mutants attenuated in plant virulence: towards phage therapy. J. Appl. Microbiol. **108**:676–685.
11. **Gabor M.** 1965. Transformation of streptomycin markers in rough strains of *Rhizobium lupini.* II. The relation between the derterminant of streptomycin dependence and those for streptomycin resistance and sensitiveness. Genetics **52**:905–913.
12. **Götz R, Limmer N, Ober K, Schmitt R.** 1982. Motility and chemotaxis in two strains of *Rhizobium* with complex flagella. J. Gen. Microbiol. **128**: 789–798.
13. **Guerrero-Ferreira RC, et al.** 2011. Alternative mechanism for bacteriophage adsorption to the motile bacterium *Caulobacter crescentus.* Proc. Natl. Acad. Sci. U. S. A. **108**:9963–9968.
14. **Higuchi R.** 1989. Using PCR to engineer DNA, p 61–70. *In* Erlich HA (ed), PCR technology. Principles and applications for DNA amplification. Stockton Press, New York, NY.
15. **Iino T, Mitani M.** 1967. Infection of *Serratia marcescens* by bacteriophage chi. J. Virol. **1**:445–447.
16. **Iino T, Mitani M.** 1967. A mutant of *Salmonella* possessing straight flagella. J. Gen. Microbiol. **49**:81–88.
17. **Kamberger W.** 1979. An Ouchterlony double diffusion study on the interaction between legume lectins and rhizobial cell surface antigens. Arch. Microbiol. **121**:83–90.
18. **Krupski G, Götz R, Ober K, Pleier E, Schmitt R.** 1985. Structure of complex flagellar filaments in *Rhizobium meliloti.* J. Bacteriol. **162**:361–366.
19. **Lotz W, Acker G, Schmitt R.** 1977. Bacteriophage 7-7-1 adsorbs to the complex flagella of *Rhizobium lupini* H13-3. J. Gen. Virol. **34**:9–17.
20. **Lotz W, Mayer F.** 1972. Electron microscopical characterization of newly isolated *Rhizobium lupini* bacteriophages. Can. J. Microbiol. **18**:1271–1274.
21. **Macnab RM.** 1996. Flagella and motility, p 123–145. *In* Neidhardt FC, et al (ed), *Escherichia coli* and *Salmonella*: cellular and molecular biology, vol 1. ASM Press, Washington, DC.
22. **Macnab RM, Ornston MK.** 1977. Normal-to-curly flagellar transitions and their role in bacterial tumbling. Stabilization of an alternative quaternary structure by mechanical force. J. Mol. Biol. **112**:1–30.
23. **Manson MD, Tedesco P, Berg HC, Harold FM, Van der Drift C.** 1977. A protonmotive force drives bacterial flagella. Proc. Natl. Acad. Sci. U. S. A. **74**:3060–3064.
24. **Meier VM, Muschler P, Scharf BE.** 2007. Functional analysis of nine putative chemoreceptor proteins in *Sinorhizobium meliloti.* J. Bacteriol. **189**:1816–1826.
25. **Novick RP, et al.** 1976. Uniform nomenclature for bacterial plasmids: a proposal. Bacteriol. Rev. **40**:168–189.
26. **Petty NK, Foulds IJ, Pradel E, Ewbank JJ, Salmond GP.** 2006. A generalized transducing phage (phiIF3) for the genomically sequenced *Serratia marcescens* strain Db11: a tool for functional genomics of an opportunistic human pathogen. Microbiology **152**:1701–1708.
27. **Platzer J, Sterr W, Hausmann M, Schmitt R.** 1997. Three genes of a motility operon and their role in flagellar rotary speed variation in *Rhizobium meliloti.* J. Bacteriol. **179**:6391–6399.
28. **Raimondo LM, Lundh NP, Martinez RJ.** 1968. Primary adsorption site of phage PBS1: the flagellum of *Bacillus subtilis.* J. Virol. **2**:256–264.
29. **Randall-Hazelbauer L, Schwartz M.** 1973. Isolation of the bacteriophage lambda receptor from *Escherichia coli.* J. Bacteriol. **116**:1436–1446.
30. **Ravid S, Eisenbach M.** 1983. Correlation between bacteriophage chi adsorption and mode of flagellar rotation of *Escherichia coli* chemotaxis mutants. J. Bacteriol. **154**:604–611.
31. **Samuel AD, et al.** 1999. Flagellar determinants of bacterial sensitivity to chi-phage. Proc. Natl. Acad. Sci. U. S. A. **96**:9863–9866.
32. **Schade SZ, Adler J, Ris H.** 1967. How bacteriophage chi attacks motile bacteria. J. Virol. **1**:599–609.
33. **Schäfer A, et al.** 1994. Small mobilizable multi-purpose cloning vectors derived from the *Escherichia coli* plasmids pK18 and pK19: selection of defined deletions in the chromosome of *Corynebacterium glutamicum.* Gene **145**:69–73.
34. **Scharf B.** 2002. Real-time imaging of fluorescent flagellar filaments of *Rhizobium lupini* H13-3: flagellar rotation and pH-induced polymorphic transitions. J. Bacteriol. **184**:5979–5986.
35. **Scharf B, Schuster-Wolff-Bühring H, Rachel R, Schmitt R.** 2001. Mutational analysis of *Rhizobium lupini* H13-3 and *Sinorhizobium meliloti* flagellin genes: importance of flagellin A for flagellar filament structure and transcriptional regulation. J. Bacteriol. **183**:5334–5342.
36. **Schmitt R, Raska I, Mayer F.** 1974. Plain and complex flagella of *Pseudomonas rhodos*: analysis of fine structure and composition. J. Bacteriol. **117**:844–857.
37. **Simon R, O'Connell M, Labes M, Pühler A.** 1986. Plasmid vectors for the genetic analysis and manipulation of rhizobia and other gram-negative bacteria. Methods Enzymol. **118**:640–659.
38. **Simon R, Priefer U, Pühler A.** 1983. A broad host range mobilisation system for *in vivo* genetic engineering: transposon mutagenesis in gram negative bacteria. Biotechnology (NY) **1**:783–791.
39. **Skurray RA, Hancock RE, Reeves P.** 1974. Con-mutants: class of mutants

in *Escherichia coli* K-12 lacking a major cell wall protein and defective in conjugation and adsorption of a bacteriophage. J. Bacteriol. **119**:726–735.
40. **Sourjik V, Schmitt R.** 1996. Different roles of CheY1 and CheY2 in the chemotaxis of *Rhizobium meliloti.* Mol. Microbiol. **22**:427–436.
41. **Thienel P.** 1977. Morphologie, DNA-Structur und Adsorptionskinetik des flagellotropen Phagen 7-7-1 an *Rhizobium lupini* H13-3. Universität Regensburg, Regensburg, Germany.
42. **Trachtenberg S, DeRosier DJ, Aizawa S, Macnab RM.** 1986. Pairwise perturbation of flagellin subunits. The structural basis for the differences between plain and complex bacterial flagellar filaments. J. Mol. Biol. **190**: 569–576.
43. **Trachtenberg S, DeRosier DJ, Macnab RM.** 1987. Three-dimensional structure of the complex flagellar filament of *Rhizobium lupini* and its relation to the structure of the plain filament. J. Mol. Biol. **195**:603–620.
44. **Wibberg D, et al.** 2011. Complete genome sequencing of *Agrobacterium* sp. H13-3, the former *Rhizobium lupini* H13-3, reveals a tripartite genome consisting of a circular and a linear chromosome and an accessory plasmid but lacking a tumor-inducing Ti-plasmid. J. Biotechnol. **155**:50–62.
45. **Wolfe AJ, Berg HC.** 1989. Migration of bacteria in semisolid agar. Proc. Natl. Acad. Sci. U. S. A. **86**:6973–6977.